Dynamic Downscaling of the North American Monsoon with the NCEP–Scripps Regional Spectral Model from the NCEP CFS Global Model

STEVEN C. CHAN

Center for Ocean–Atmospheric Prediction Studies, The Florida State University, Tallahassee, Florida

VASUBANDHU MISRA

Center for Ocean–Atmospheric Prediction Studies, and Department of Earth, Ocean, and Atmospheric Science, The Florida State University, Tallahassee, Florida

(Manuscript received 22 December 2009, in final form 27 July 2010)

ABSTRACT

The June–September (JJAS) 2000–07 NCEP coupled Climate Forecasting System (CFS) global hindcasts are downscaled over the North and South American continents with the NCEP–Scripps Regional Spectral Model (RSM) with anomaly nesting (AN) and without bias correction (control). A diagnosis of the North American monsoon (NAM) in CFS and RSM hindcasts is presented here. RSM reduces errors caused by coarse resolution but is unable to address larger-scale CFS errors even with bias correction. CFS has relatively weak Great Plains and Gulf of California low-level jets. Low-level jets are strengthened from downscaling, especially after AN bias correction. The RSM NAM hydroclimate shares similar flaws with CFS, with problematic diurnal and seasonal variability. Flaws in both diurnal and monthly variability are forced by erroneous convection-forced divergence outside the monsoon core region in eastern and southern Mexico. NCEP reanalysis shows significant seasonal variability errors, and AN shows little improvement in regional-scale flow errors. The results suggest that extreme caution must be taken when the correction is applied relative to reanalyses. Analysis also shows that North American Regional Reanalysis (NARR) NAM seasonal variability has benefited from precipitation data assimilation, but many questions remain concerning NARR's representation of NAM.

1. Introduction

The North American monsoon (NAM) is one of the most important features of the North American climate (Adams and Comrie 1997; Higgins and Gochis 2007). The monsoon extends from northwest Mexico along the Sierra Madre Occidental (SMO) to the Basin and Range Province in the southwestern United States. The highest precipitation is observed over the Mexican SMO and decreases northward into the southwestern United States. The central focus of this study is the Tier 1 (20°–35°N, 105°–115°W) and Tier 2 (10°–40°N, 90°–120°W) boxes of the North American Monsoon Experiment (NAME; Higgins and Gochis 2007).

NAME (Higgins and Gochis 2007) is a multi-institutional project that aims to increase knowledge and understanding of the NAM. The program includes an intensive field campaign in the 2004 boreal summer NAM season with aircraft–ship observations, radiosonde soundings, and radar–rain gauge measurements that can be compared with other independent climate and satellite datasets (Higgins and Gochis 2007; Gochis et al. 2007; Zuidema et al. 2007; Nesbitt et al. 2008). The NAME modeling assessments (NAMAP and NAMAP2) explore global and regional model skill in simulating NAM—its seasonal, intraseasonal, and diurnal variability—and identify areas for improvement in the models (Collier and Zhang 2007; Gao et al. 2007; Lee et al. 2007; Gutzler et al. 2009).

The observed NAM season occurs during July and August, with a dry June premonsoon and a September retreat (Adams and Comrie 1997). Synoptic weather systems play an important role in NAM intraseasonal variability (Douglas and Englehart 2007). Pre-NAME in situ

Corresponding author address: Dr. Steven C. Chan, FSU Center for Ocean–Atmospheric Prediction Studies, 2035 East Paul Dirac Dr., Room 200, Johnson Building, Tallahassee, FL 32308.
E-mail: schan@fsu.edu

DOI: 10.1175/2010JCLI3593.1

diurnal observations of diurnal NAM variations are scarce; NAME in situ radar and rain gauge measurements combined with satellite measurements show that precipitation develops initially in the elevated terrain in the afternoon–early evening and moves toward the Pacific Coast and the Gulf of California (GC) overnight (Janowiak et al. 2007; Becker and Berbery 2008; Nesbitt et al. 2008; Johnson et al. 2010).

The accurate simulation of NAM in global climate models is a challenging science problem. Seasonal variability—the very definition of the word "monsoon"—is often erroneously simulated in these models. Yang et al. (2009) found that in the National Centers for Environmental Prediction (NCEP) Climate Forecasting System (CFS) boreal summer NAM rainfall in the southwestern United States peaks later than observed with excessive boreal winter precipitation. Likewise, Collier and Zhang (2007) found similar issues with the National Center for Atmospheric Research (NCAR) Community Atmosphere Model, version 3 (CAM3) simulations forced with observed SST. These studies also showed that CFS and CAM3 seasonal cycles are highly sensitive to horizontal resolution. However, higher resolution does not necessarily improve the simulated seasonal cycle. In fact, the higher-resolution version of the models further exacerbates the excessive boreal winter precipitation (Collier and Zhang 2007; Yang et al. 2009). For the diurnal cycle, Janowiak et al. (2007) found that operational models tend to have diurnal precipitation peaking too early. Lee et al. (2007) found that the diurnal cycle of precipitation in the global model improves with increased horizontal resolution over the Rockies, the SMO, and coastal areas.

Anderson and Roads (2002) downscaled the Scripps Global Spectral Model with the NCEP–Scripps Regional Spectral Model (RSM; Juang and Kanamitsu 1994) over the southwestern United States. Comparisons with surface observations show that RSM is able to simulate realistic intraseasonal (Anderson 2002) and diurnal (Anderson and Kanamaru 2005) precipitation variations in this region. The RSM hydroclimate shows the southwestern United States is a net moisture source region with moisture flux divergences above the planetary boundary layer (PBL) exceeding the low-level moisture flux convergences (Anderson and Kanamaru 2005; Anderson et al. 2004).

This study seeks to investigate the feasibility of downscaling over the NAM region from the NCEP CFS (Saha et al. 2006) for routine operational seasonal prediction using the NCEP–Scripps RSM. This is one of the first attempts to downscale a global coupled ocean–atmosphere model for a seasonal predictability study over the NAM region. The following are some of the compelling reasons to pursue this downscaling study for seasonal predictability:

1) Misra and Kanamitsu (2004) demonstrated improved seasonal predictability of the South American monsoon (SAM) from anomaly nesting (AN) even when the driving global model had large biases.
2) Misra (2007) showed that the combination of scale-selective bias correction and anomaly nesting leads to further improvements in downscaled climate modeling.
3) RSM is shown to display reasonable diurnal, synoptic, and seasonal hydroclimate in part of the NAM region (Anderson and Roads 2002; Anderson et al. 2004; Anderson and Kanamaru 2005).

An earlier study by Misra (2007) has been expanded to examine the efficacy of these downscaling methodologies in the context of the NAM. Based on the results of this study, as well as the results of other similar studies, the focus here will be the seasonal (monthly) and diurnal variabilities. The details of the models and observations used are given in section 2, and a description of the AN method is provided in section 3. Comparisons between CFS, RSM, and observations are presented in sections 4–6, and the summary and discussion of the findings are given in section 7.

2. Models and data

a. The NOAA–NCEP CFS

The National Oceanic and Atmospheric Administration (NOAA)–NCEP CFS (Saha et al. 2006) is a fully coupled ocean–land–atmosphere global climate model. The T62 ($\sim 1.875° \times 1.875°$) spectral model has 64 vertical sigma levels. We have used the "frozen" version of CFS with the simplified Arakawa–Schubert cumulus convection (SAS; Hong and Pan 1998), NCEP medium-range forecast PBL scheme (Hong and Pan 1996), and the Oregon State University land surface scheme (Mahrt and Pan 1984). CFS is used to investigate the NAM during the 2004 NAME field experiment year (Gutzler et al. 2009) and the southwestern United States warm season (Yang et al. 2009).

Six ensemble member CFS seasonal hindcasts are carried out for June–September (JJAS) of 2000–07 (for a total of 48 simulations). The ensemble members are generated by perturbing the initial state of the atmosphere. The six atmospheric initial conditions for a given year are generated by resetting the initial date of the atmospheric restart file after integrating CFS for a week from the NCEP–NCAR reanalysis (NRR); the procedure was then repeated to obtain the required number of initial states. This methodology was successfully implemented in earlier studies to generate synoptically independent initial conditions (Kirtman et al. 2001; Misra et al. 2008). The ocean and land initial states are identical in all six ensemble members. The ocean initial state is obtained from the Global Ocean Data Assimilation System (GODAS; Behringer and Xue 2004), and the initial land surface conditions are from the NCEP–Department of Energy (DOE) reanalysis II (Kanamitsu et al. 2002). The start date of the integrations was at 0000 UTC 23 May for all years from 2000 to 2007. Upper-atmosphere outputs are available at 6-h intervals; single-level outputs are available as daily averages.

b. The NCEP–Scripps RSM

The NCEP–Scripps RSM has undergone significant changes since its introduction (Juang and Kanamitsu 1994). Subsequent updates include the scale-selective bias correction (SSBC; Kanamaru and Kanamitsu 2007). The SSBC involves nudging the vorticity in spectral space within the regional domain on wavelengths larger than 1000 km and forcing domain mean temperature perturbations to zero. Besides reducing the drift of the regional climate model, the SSBC removes the need for multiple nesting to downscale to a fine grid (Kanamaru and Kanamitsu 2007).

RSM has 28 sigma vertical levels. For this study, RSM is run at a 60-km horizontal resolution. The resolution is coarser than that of some of the earlier downscaling studies (Anderson and Roads 2002; Gochis et al. 2002), but RSM is integrated over a much larger domain, covering a large fraction of the North and South American continents. In the future, we intend to compare and contrast the impact of downscaling on the winter and summer counterparts of the NAM and the SAM. The same cumulus (SAS) and PBL (NCEP medium-range forecast scheme) parameterizations are used in CFS and RSM, but a different land surface scheme is used [NCEP–Ohio State–U.S. Air Force–National Weather Service (NWS) Hydrology Laboratory (NOAH) land scheme; Ek et al. 2003]. It is known that model-simulated NAM is sensitive to cumulus parameterization (Gochis et al. 2002), and we have found SAS to work best for our simulations.

There are two sets of RSM simulations conducted in this study: one downscales directly from individual CFS ensemble members using the corresponding CFS SSTs, [hereafter referred to as control RSM (*C*) or *C* simulations], and one downscales from bias-corrected CFS outputs [the anomaly-nested (see section 3) RSM (AN) or AN simulations]. Isobaric upper-air and single-layer outputs are available at 6-h intervals.

c. The North American Regional Reanalysis

The North American Regional Reanalysis (NARR; Mesinger et al. 2006) is used as a reanalysis dataset for verification of both the coarser-grid CFS and the finer-grid RSM simulations. Unlike other global reanalyses, NARR assimilates observed precipitation, which makes it suitable for precipitation validation.

However, significant issues remain with NARR's hydroclimate. Within the context of NAM, there are four well-documented issues:

1) Surface evaporation is generally poor over continental North America (Nigam and Ruiz-Barradas 2006).
2) NARR is known to have an excessively strong GC low-level jet (GCLLJ; Mo et al. 2005).
3) The assimilation of diurnal precipitation variability outside the United States is based on reanalysis II forecasts. Within the contiguous states, assimilated diurnal variability is based on hourly rain gauge observations.
4) NARR's GC SST is set to the observed value at Guaymas, Mexico (see section 4).

d. Other observations

Numerous other observational datasets are used to carry out RSM simulations. The NCEP–NCAR reanalysis I (Kalnay et al. 1996) and the extended reconstructed SST version 2 (ERSSTv2) SSTs (Smith and Reynolds 2004) are used for the AN bias corrections. The NCEP–DOE reanalysis II land surface analysis provides the soil moisture initial conditions for both RSM and CFS.

3. The AN method

Anomaly nesting (Misra and Kanamitsu 2004) is a method for correcting biases in global model climatology before downscaling. The method removes the global model long-term seasonal mean climatology and replaces it with reanalysis climatology.

CFS JJAS climatology is replaced with the corresponding climatology from the NCEP–NCAR reanalysis I (atmosphere) and ERSSTv2 (SST) climatology over the period of 1950–95. CFS climatology is derived from the T62 33-yr multidecadal simulations (available online from the CFS Web site; see http://cfs.ncep.noaa.gov/). Atmospheric seasonal bias corrections are applied to humidity, divergence, vorticity, and temperature at all RSM vertical levels. This is a significant departure from the methodology of Misra and Kanamitsu (2004); they conducted an AN bias correction that included the diurnal variation of the atmospheric variables.

4. Land–sea contrasts and topography

An obvious difference between the higher-resolution RSM and the lower-resolution CFS is the depiction of

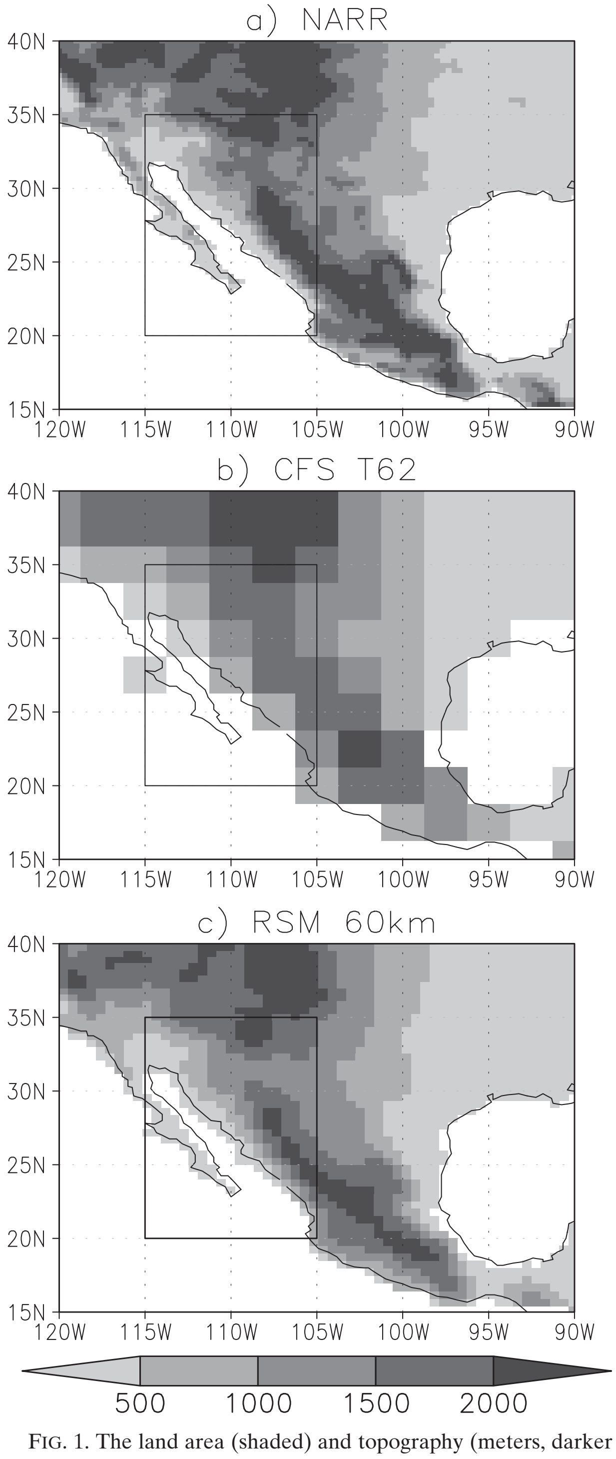

FIG. 1. The land area (shaded) and topography (meters, darker shades) for the (a) NARR, (b) NCEP CFS, and (c) NCEP–Scripps RSM.

the topography and land–sea contrasts. Both play important roles in the formation of nocturnal low-level jets (LLJs) in the Great Plains and the Gulf of California (Holton 1967). In Fig. 1, the land–sea masks and surface topographies of NARR, CFS, and RSM are shown at their native horizontal resolutions of 25, ~200, and 60 km, respectively. There are two main differences:

1) CFS land–sea geometry for the GC is unrealistic because Baja California is omitted from CFS.
2) The SMO is depicted as relatively gradual in CFS and is lower in height than in the higher-resolution RSM and NARR.

The GC in CFS is a bowl-shaped bay with Baja California appearing as a ‘‘block’’ sticking out from the mainland. Observed SSTs along the California west coast are much lower than the GC SSTs because of the Pacific Eastern Boundary Current and cannot be captured correctly in CFS. The monthly mean surface temperatures (SSTs and over land) shown in Fig. 2 further illustrate the issue raised by the CFS representation of the GC. CFS SSTs over the GC are lower than those depicted in NARR, and the SST differences between the cold California Current and the warm GC are not as well differentiated.

NARR GC surface temperatures are not without problems. GC SSTs are set to a uniform value (*monthly* pre-2004, daily afterward), the observed value at Guaymas, Mexico. That leads to the clear SST discontinuity in the GC mouth; additionally, pre-2004 there is a temporal discontinuity at the end of each month as well (Mesinger et al. 2006). A quick check of the Moderate Resolution Imaging Spectroradiometer (MODIS) *Aqua* high-resolution SSTs (Feldman and McClain 2010; data available online at http://oceancolor.gsfc.nasa.gov/) indicates that boreal summer GC SSTs show a cross-gulf gradient with higher SSTs on the east side (where Guaymas is located); this implies that NARR GC SSTs lean toward the high side. In reality, though complex, GC SSTs are critical to NAM variability (Wang and Xie 2007).

RSM (*C*) inherits some of CFS problems, most notably west of Baja California and within the GC itself, with unrealistic north–south SST gradients. AN does increase GC SSTs, especially near the mouth. It is worth noting that the AN SST bias correction is applied at the native resolution of ERSSTV2, which is 1.0° × 1.0° grid resolution.

CFS shows a lower SMO. It will be shown later that both models (CFS and RSM) have westward moisture fluxes over the Mexican Central Highlands that are comparable with NARR (Fig. 9), which implies that the details of elevated terrain over Mexico have a negligible impact on moisture transport. However, CFS land surface temperatures are more troubling; CFS has higher temperatures over the southwestern United States and elevated terrain. RSM (AN and control) surface temperatures tend to be lower than both CFS and NARR.

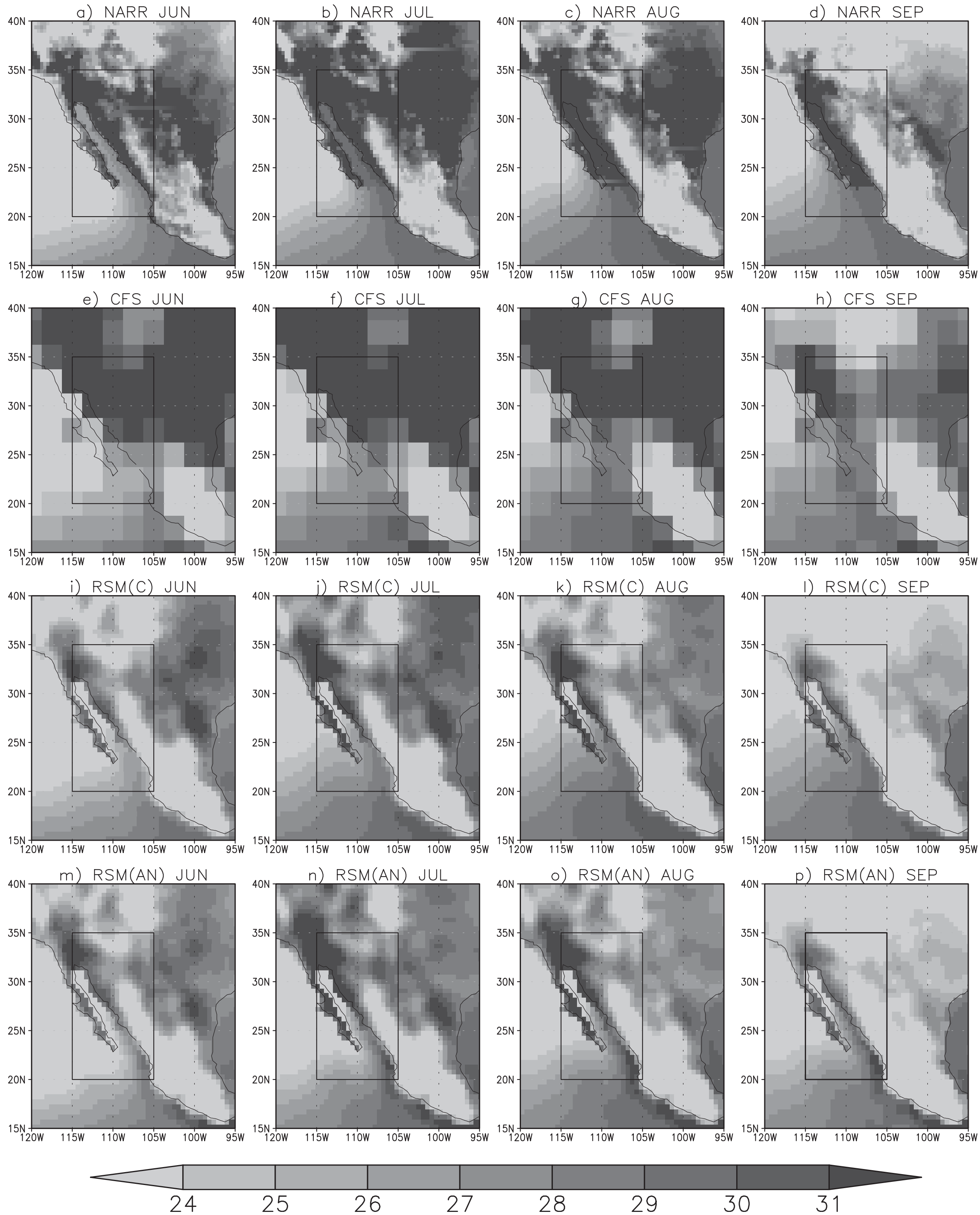

FIG. 2. The 2000–07 JJAS monthly mean surface temperatures (land and water) for (a)–(d) NARR, (e)–(h) CFS, (i)–(l) RSM (*C*), and (m),(n) RSM (AN).

5. Regional-scale NAM precipitation and atmospheric flows in different time scales

a. Precipitation

Precipitation is difficult to handle in numerical modeling, but it is often the most important value to simulate accurately. The 2000–07 JJAS monthly precipitation for NARR and the models, the seasonal differences among them, and the month-to-month changes are shown in Figs. 3, 4, and 5, respectively.

Seasonally, precipitation biases are relatively small inside the NAME Tier 1 core region and the southwestern United States, but there are much larger discrepancies in the Gulf of Mexico and farther southeast in Central America. Outside of the NAM core region in southern–eastern Mexico, CFS shows a large positive precipitation bias in excess of 7 mm day^{-1}. RSM perpetuates this erroneous bias. The simulated precipitation in southern–eastern Mexico is more intense than the monsoon precipitation. Generally, RSM and CFS precipitation biases are similar, except for the Great Plains region.

The CFS and RSM simulations capture the observed drier period before the NAM July–August peak. NAM land precipitation increases during July, consistent with NARR precipitation. However, the bulk of the simulated increase in the ‘‘CFS NAM’’ (Fig. 5), like the mean precipitation bias in Fig. 4, is centered southeast of the observed Sonora and Sinaloa core regions.

NARR monsoon precipitation over land retreats during September. Although CFS precipitation does decrease where the bulk of the seasonal precipitation maximum is located, there is little change farther north in the southwestern United States and Sonora region, consistent with the findings of Yang et al. (2009). RSM control and AN simulations share the same problem: precipitation decreases to the southeast outside of the core region, but precipitation in Sonora and the southwestern United States continues to increase in September. Southward from the GC mouth along the coastline, seasonal precipitation variability of the reanalyses and the model are in agreement. Simulated precipitation biases over the tropical–subtropical eastern Pacific are generally much less than over land (inside and outside the NAM region) and over the Gulf of Mexico.

Inside the Tier 1 box, RSM (*C*) and RSM (AN) show negative bias on the windward side of the SMO. It is conjectured that the precipitation bias in CFS is relatively small owing to the erroneously smoothed (or coarse) representation of the local orography in CFS (Fig. 1; note the absence of coastal lowlands in Mexico's Sonora state in CFS). On the other hand, the coastal lowlands are explicitly resolved by RSM. Observed precipitation in the Sonora coastal lowlands is closely linked with NAM diurnal variability (see section 1). We will argue in this paper that erroneous CFS large-scale climate has a negative influence on regional-scale climate that is resolvable by RSM (but not by CFS) in both diurnal and monthly time scales.

b. Upper-tropospheric circulations

The 200-hPa circulation and winds can be seen as an integrated measure of tropospheric temperatures and divergent circulation, especially in regions where deep convection is dominating the precipitation generation mechanism. The monthly 200-hPa geopotential heights and winds are shown in Fig. 6; ridges are marked with H. CFS- and RSM-simulated 200-hPa height seasonal variabilities are generally consistent with those of NARR. Note the double ridges in the models.

CFS and RSM (both control and AN) simulations capture the movement of the 200-hPa monsoon ridge, the ‘‘northern ridge,’’ in July and August. CFS 200-hPa height gradients are not as tight as the height gradients in NARR poleward of 35°N. This means that CFS heights for the southwestern United States are relatively high, which is consistent with the lack of precipitation retreat over the same area (Fig. 5). Evidence for the excessive seasonal total of precipitation for southern–eastern Mexico is apparent. The erroneous 200-hPa ‘‘southern’’ ridge in southern–eastern Mexico during August and September is clearly linked with excessive convection over the same area. Because of this ridge, CFS wind directions are reversed to westerly over the NAM core. This reversal is not as clear in RSM.

c. Erroneous convection, diurnal variability, and forcing to regional circulations

Convective precipitation is diurnal, so convection-forced divergent flow will exhibit diurnal variations as well. To illustrate this point, the 6-hourly diurnal variations of precipitation and 200-hPa winds are shown in Figs. 7 and 8.[1]

Within the NAM core region, NARR- and RSM-simulated (control or AN) NAM precipitation peaks in the late afternoon to overnight hours (0000–1200 UTC), consistent with NAME in situ and remote sensing measurements (Janowiak et al. 2007; Becker and Berbery 2008; Nesbitt et al. 2008; Johnson et al. 2010). There are, however, two important differences that exist between NARR and RSM. The first and obvious difference is that

[1] Six-hourly precipitation for CFS is not available for analysis because of the lack of six-hourly CFS surface field outputs; only RSM and NARR precipitation are shown in Fig. 7. However, CFS diurnal variations of upper-level winds (Fig. 8) reflect the diurnal precipitation.

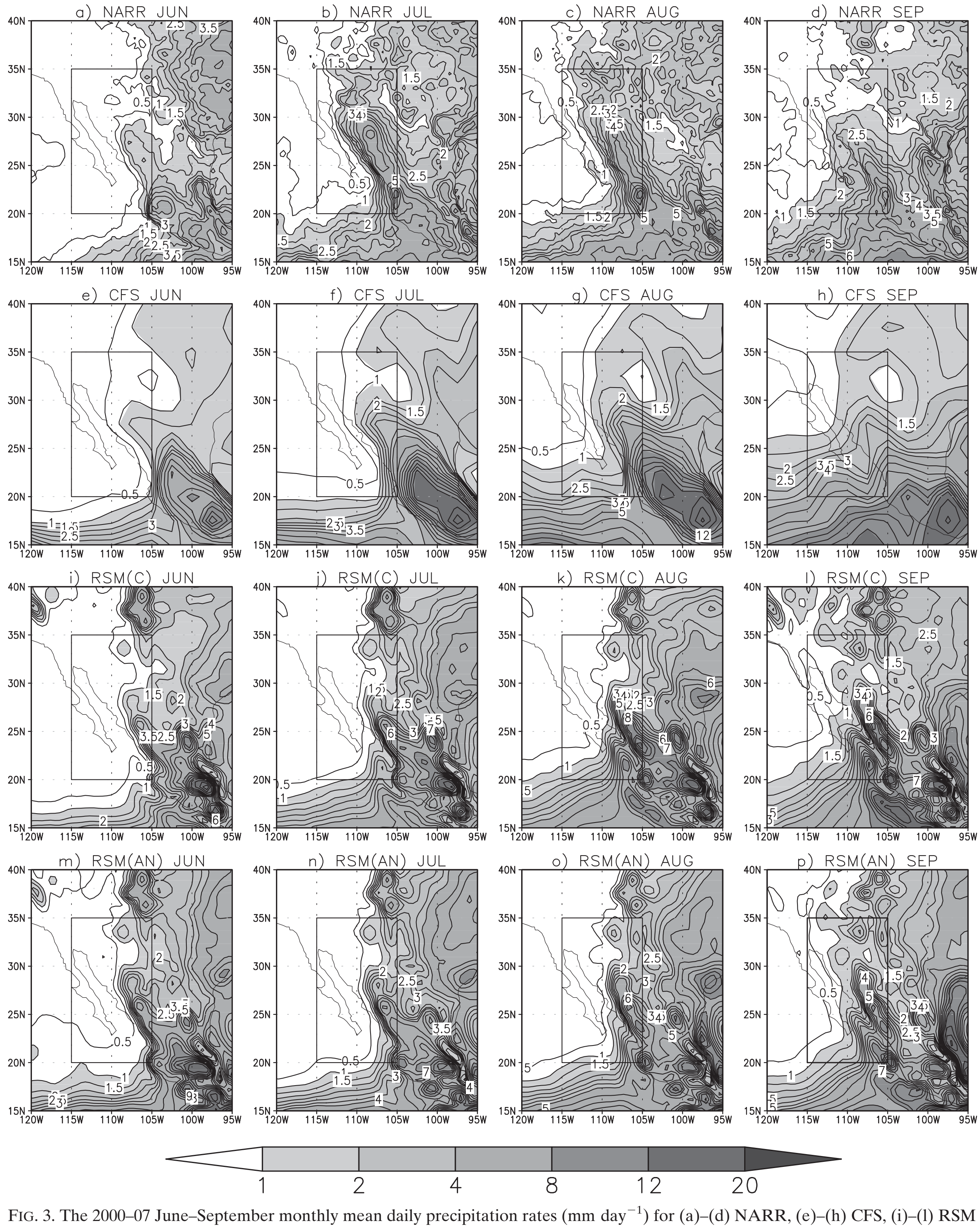

FIG. 3. The 2000–07 June–September monthly mean daily precipitation rates (mm day^{-1}) for (a)–(d) NARR, (e)–(h) CFS, (i)–(l) RSM (*C*), and (m)–(o) RSM (AN). The NAME Tier 1 region is marked with a rectangle.

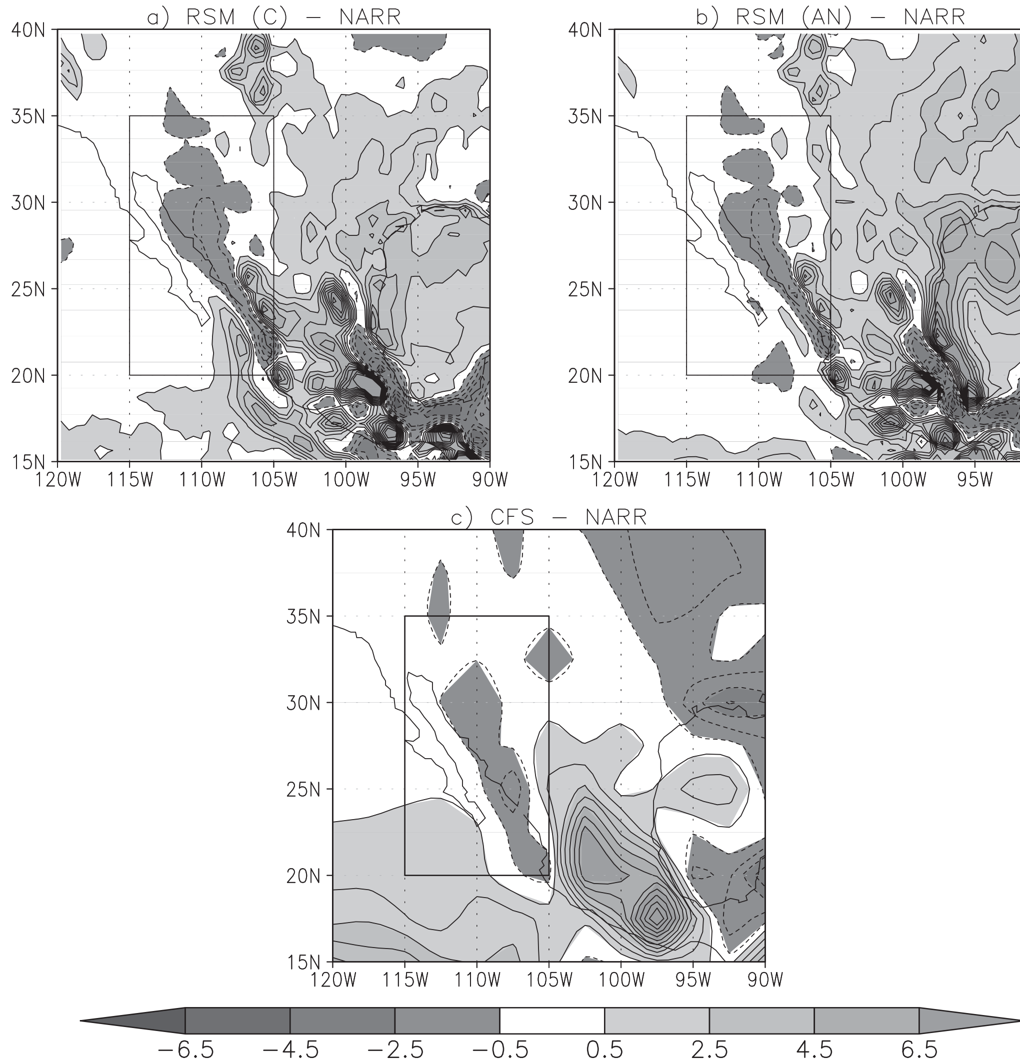

FIG. 4. The JJAS seasonal precipitation differences between the models and NARR: (a) RSM (*C*) minus NARR; (b) RSM (AN) minus NARR; and (c) CFS minus NARR. Contour intervals are every 1 mm day^{-1}.

NARR NAM diurnal precipitation develops and ends earlier than that of RSM. Considering observed uncertainties and our lack of 3-hourly RSM outputs, RSM diurnal variation of precipitation intensity seems reasonable.[2]

The second, more subtle and more important difference between NARR and RSM is the diurnal movement of the precipitation. Agreeing with observations, NARR precipitation has a clear signal of moving toward the GC from onset (1800 UTC, ~local noon) toward midnight (0600 UTC, ~local midnight). However, RSM precipitation moves both ways, toward GC and inland, with the bulk moving *inland* (northeastward). The erroneous RSM diurnal movement of precipitation is consistent with the seasonal bias over the coastal lowlands (Fig. 4); if the model fails to capture convection moving off the SMO toward the coastal lowlands and GC, then there will be negative precipitation bias over the coastal lowlands and GC.

The simulated erroneous seasonal convection farther southeast outside the NAME core shows a clear diurnal variation, peaking near 0000 UTC (local later afternoon–evening). The upper-level winds respond to that diurnal forcing. Nocturnal 200-hPa outflow develops around 0000 UTC and lasts until 0600 UTC, and clear CFS and RSM 200-hPa westerlies develop over the NAM core region. This outflow westerly forcing coincides with the simulated NAM precipitation, which moves erroneously

[2] There is a 3–6-h spread in the timing of maximum diurnal precipitation between gauge and remote sensing measurements (Nesbitt et al. 2008).

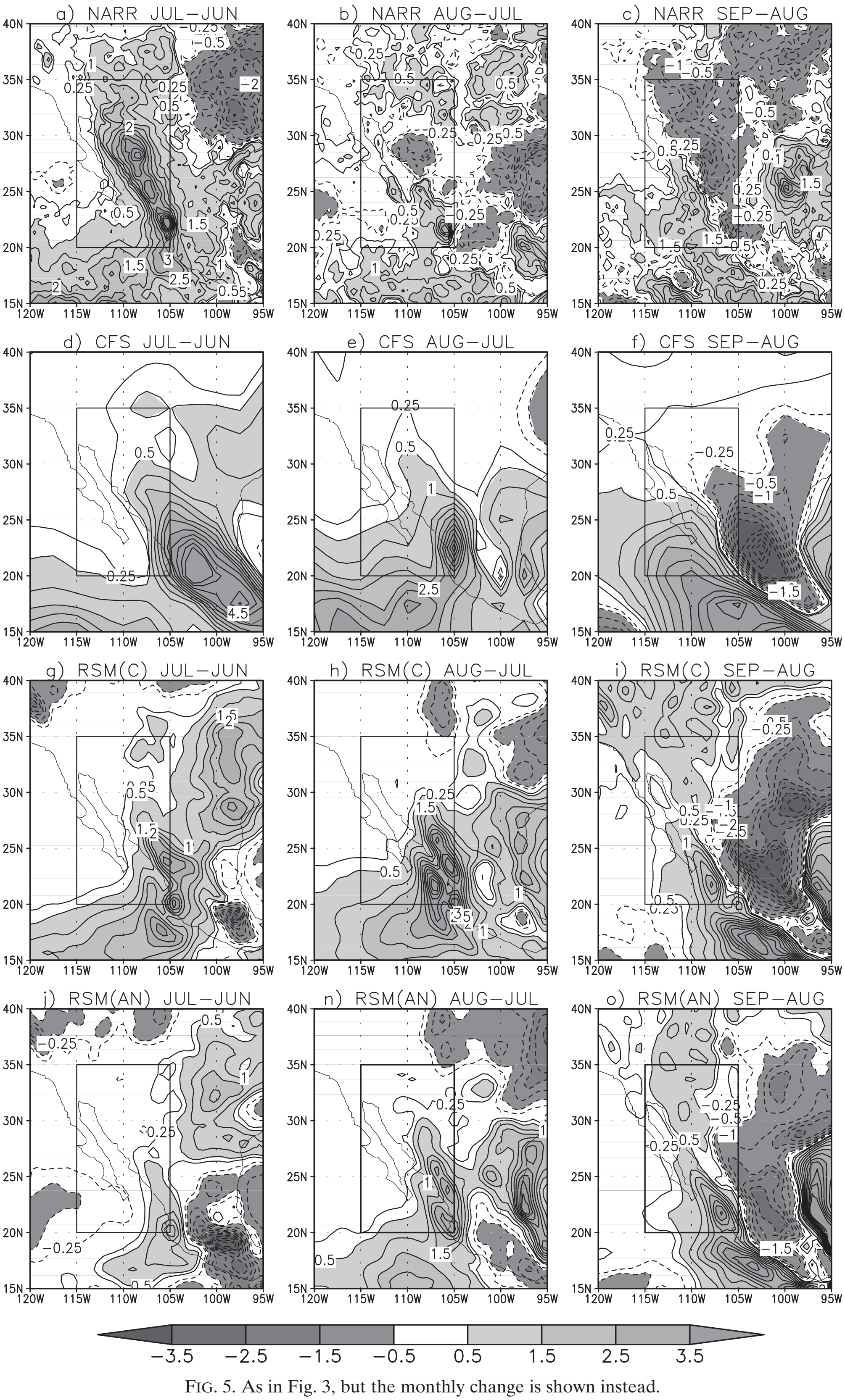

FIG. 5. As in Fig. 3, but the monthly change is shown instead.

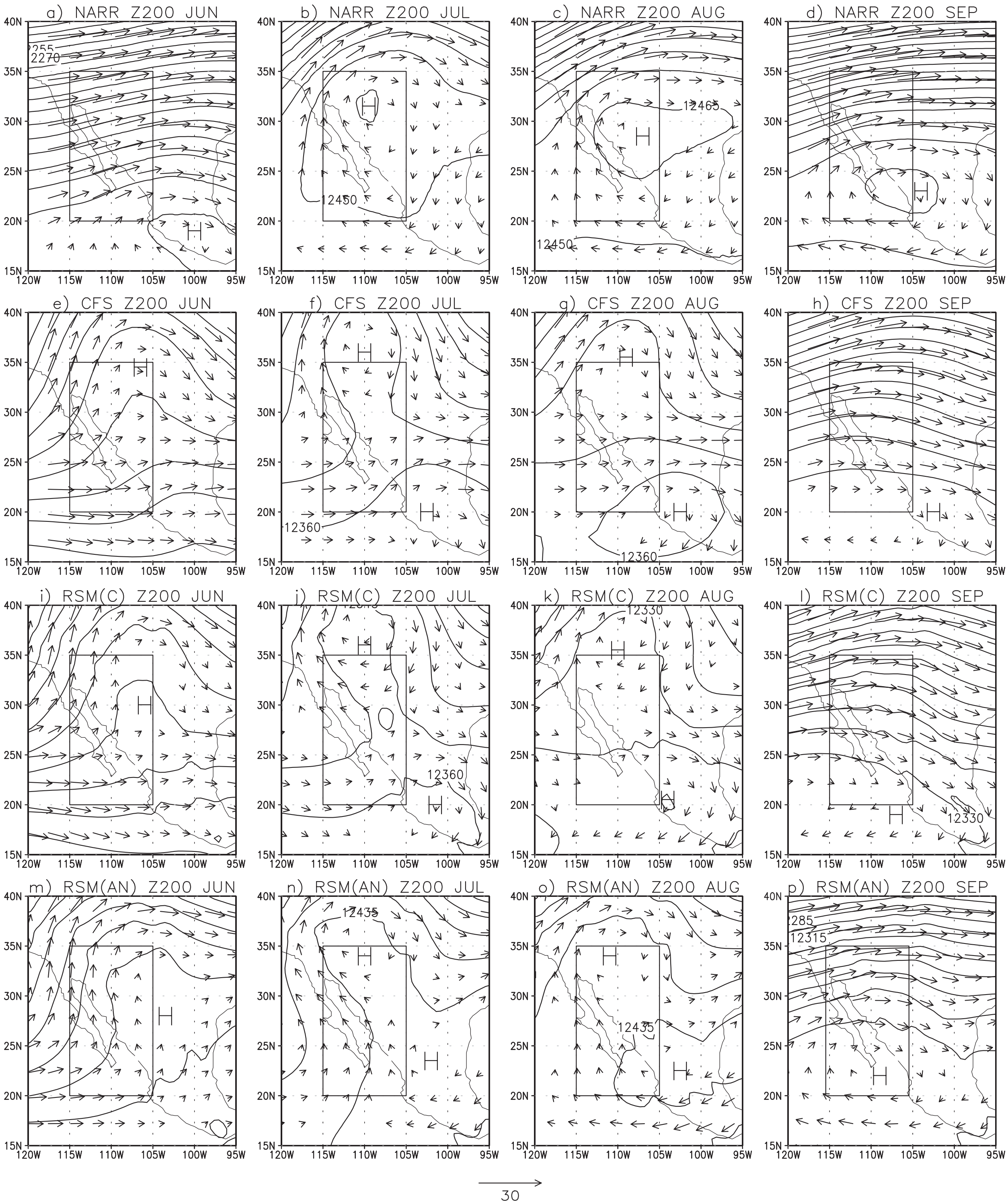

FIG. 6. Similar to Fig. 2, but 200-hPa geopotential heights and winds are shown instead. Contour intervals are every 15 m. The letter *H* marks ridge centers.

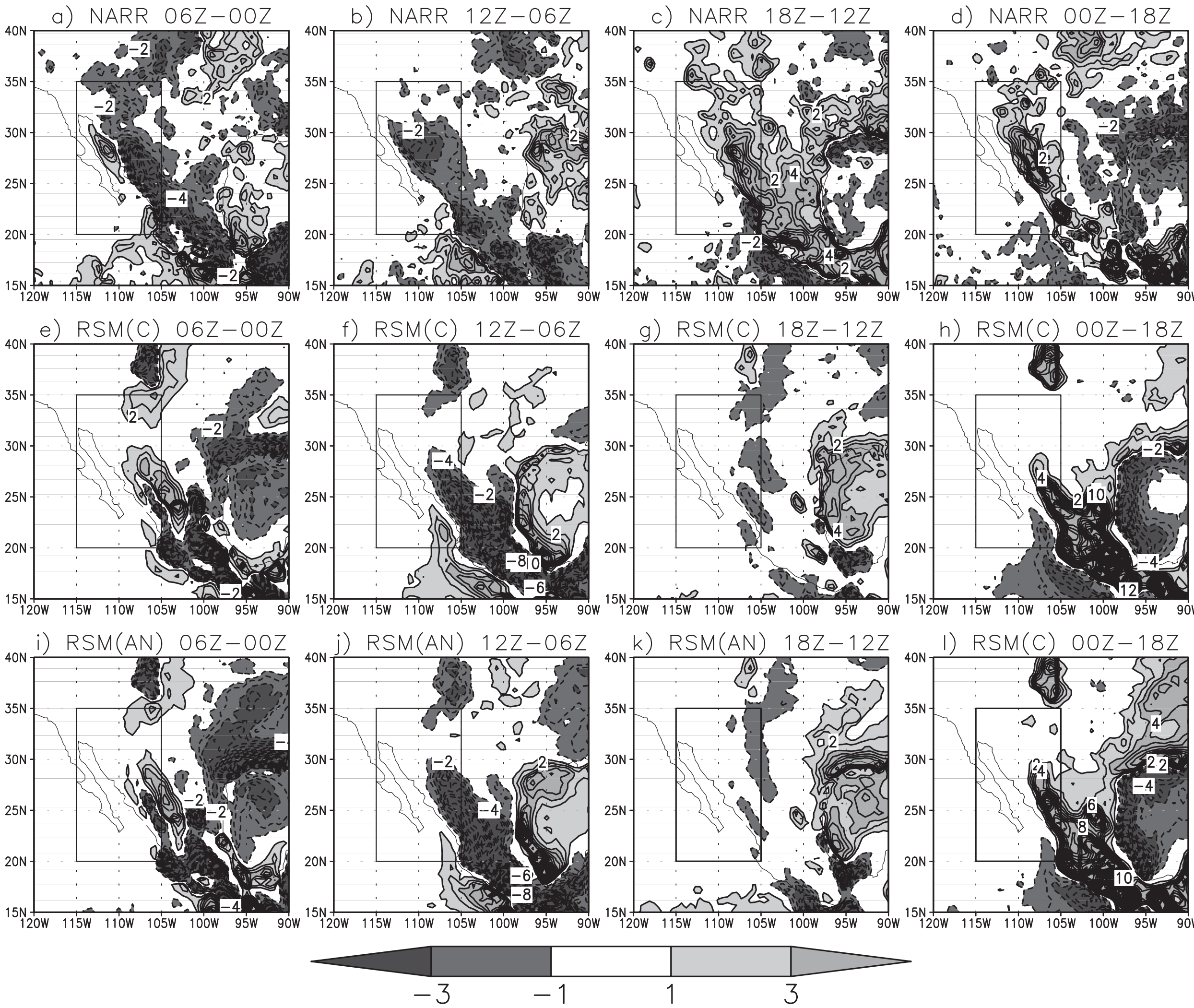

FIG. 7. The change of precipitation every 6 h (in UTC) in August of NARR and the models. Contour intervals are every 1 mm day^{-1}. Here, 0000, 0600, 1200, and 1800 UTC correspond to 1600–1800, 2200–0000, 0400–0600, and 1000–1200 local time in central Mexico and the southwest United States.

according to the diurnal forcing. When the simulated diurnal precipitation subsides during the dawn hours (1200 UTC), CFS and RSM 200-hPa winds converge over the area where the erroneous convection was 12 h earlier. In summary, the model-simulated diurnal and monthly variabilities are fundamentally connected.

6. NAM moisture fluxes and their implications

From the perspective of seasonal precipitation and its diurnal variations, the merit of downscaling (control or AN) may not be readily apparent. There are expectations that the two low-level jets—the weaker GCLLJ and the stronger Great Plains low-level jet (GPLLJ) (Higgins and Gochis 2007)—would be better resolved by the regional model. Here, the LLJs will be represented in terms of their moisture fluxes. Both atmospheric moisture and LLJs maximize in the lower troposphere. A moisture flux representation provides an integrated picture of the strength of LLJs and their roles in the hydroclimate.

Applying Reynolds decomposition, the monthly mean moisture fluxes are decomposed into overbar stationary and primed transient components [Eq. (1)]:

$$\overline{q\mathbf{V}} = \overline{q}\overline{\mathbf{V}} + \overline{q'\mathbf{V}'}. \tag{1}$$

Assuming hydrostatic balance, the mass-weighted vertical (from the surface to the 150-hPa isobar) integrated flux is

$$\int_{z_{sfc}}^{z_{150}} \overline{\rho}\,\overline{q}\overline{\mathbf{V}}\,dz = g\int_{P_{sfc}}^{150} \overline{q}\overline{\mathbf{V}}\,dp = \mathbf{F} \quad \text{and} \tag{2}$$

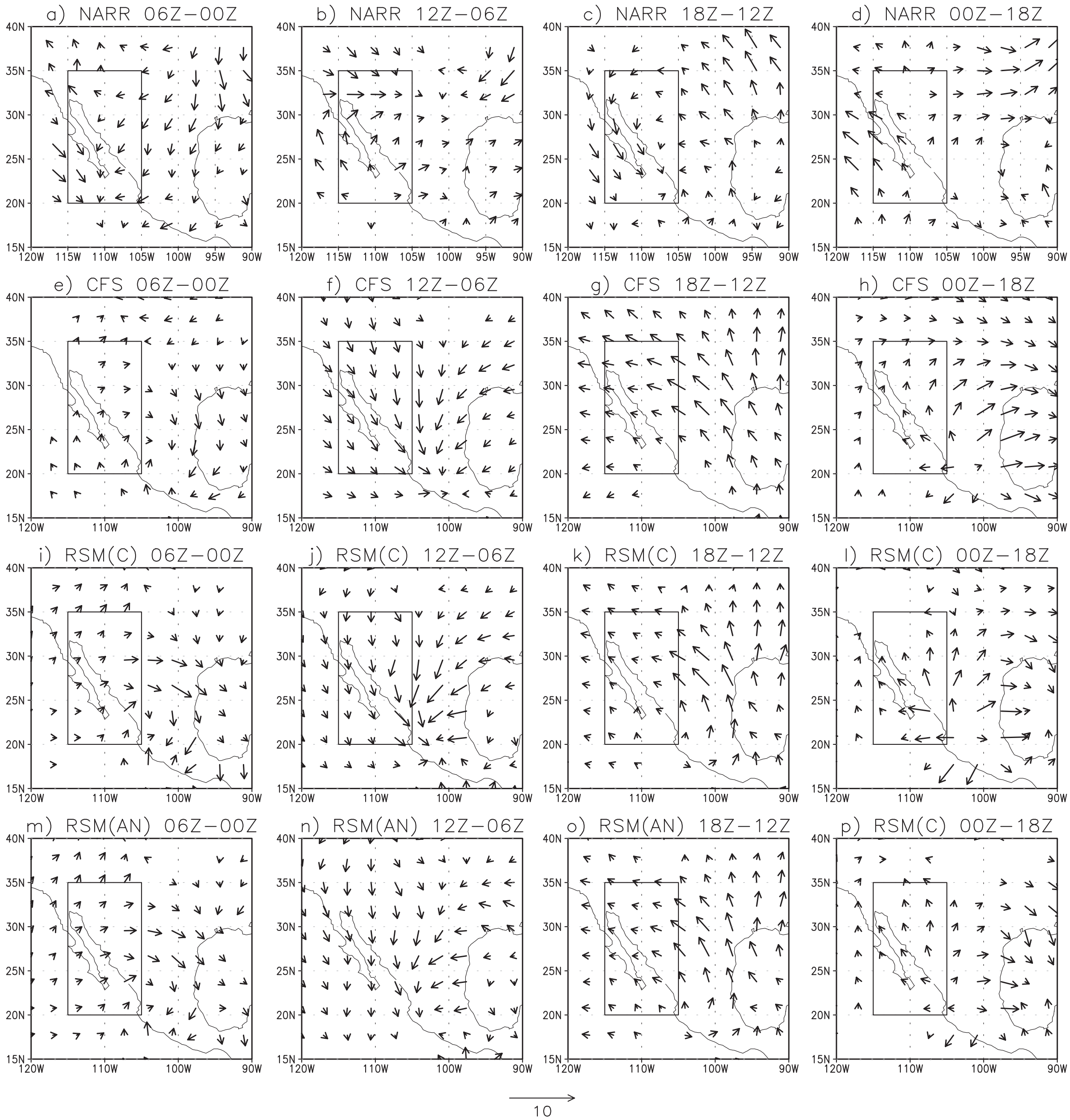

FIG. 8. As in Fig. 7, but 200-hPa wind vectors are shown instead. The vector scale is marked at the bottom.

$$\int_{z_{sfc}}^{z_{150}} \overline{\rho}\,\overline{q'\mathbf{V}'}\,dz = g\int_{P_{sfc}}^{150} \overline{q'\mathbf{V}'}\,dp = \mathbf{f}. \qquad (3)$$

a. LLJ moisture fluxes and monthly variability

The NARR and simulated meridional components of total vertical integral moisture fluxes–$[(\mathbf{F} + \mathbf{f}) \cdot \mathbf{j}]$–are shown in Fig. 9; Fig. 10 shows the month-to-month changes to highlight NARR and modeled seasonal variability. To compare the results of the current study with the results of an earlier study, readers are referred to Fig. 13 in Mo et al. (2005).

The strongest NARR and RSM poleward moisture fluxes are found within the monsoon core region, the Great Plains, and western Texas. Mo et al. (2005) showed that NARR GCLLJ is grossly overestimated, with GCLLJ moisture fluxes possibly twice as much as they really are. NARR GCLLJ continues to strengthen in

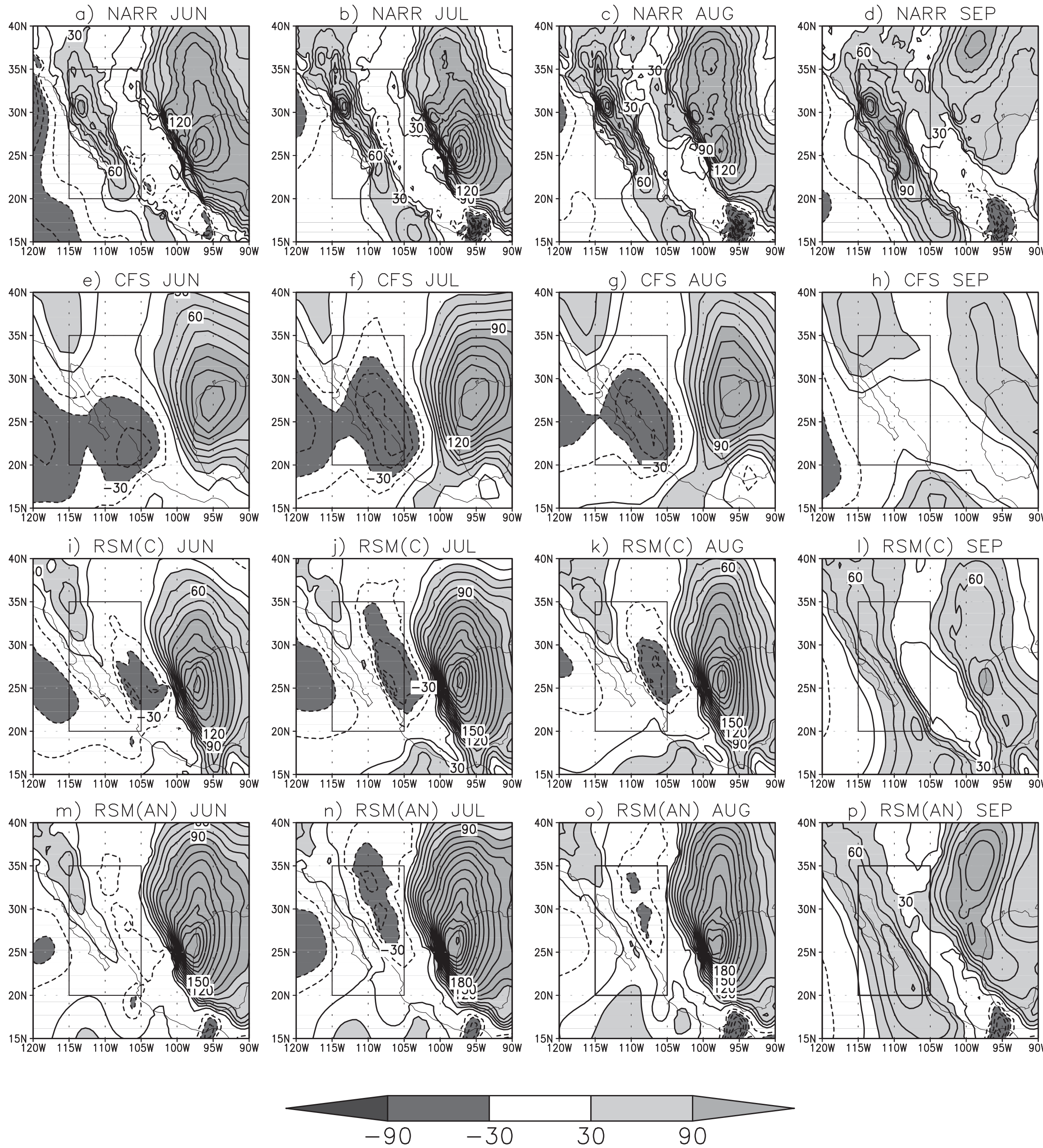

FIG. 9. The June–September meridional component of monthly mass-weighted surface to 125-hPa vertical-integrated stationary plus transient $[(\mathbf{F} + \mathbf{f}) \cdot \mathbf{j}]$ moisture fluxes (kg s^{-1} m^{-1}). (bottom) The scale of the vector is shown.

September, and deep tropical eastern Pacific moisture continues to be fueled into the NAM core region; in reality, this may be untrue (Fig. 9 in Mo et al. 2005). CFS ''GCLLJ'' moisture fluxes are *equatorward* moisture fluxes through August. The RSM-simulated GCLLJ moisture fluxes show a significant improvement over those of CFS. Both control- and AN-simulated poleward GCLLJ fluxes are weaker than those of NARR, and the AN fluxes are relatively stronger. This implies that RSM GCLLJs are more realistic than those of NARR.

Unlike NARR GCLLJ, NARR GPLLJ is more realistic (Mo et al. 2005). RSM improvement is seen clearly

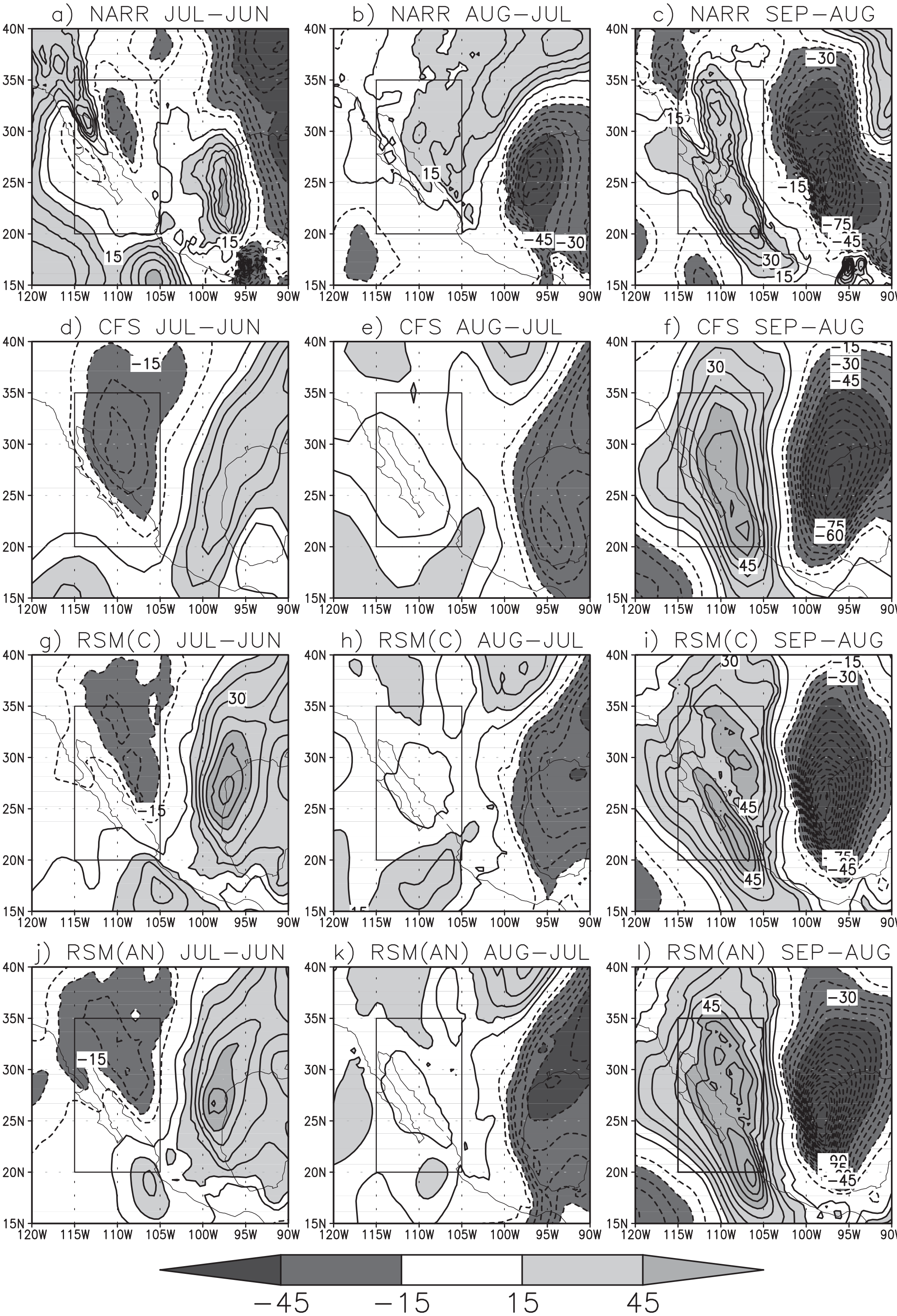

FIG. 10. Similar to Fig. 9, but the monthly differences are shown instead.

in GPLLJ, where both RSM control- and AN-simulated GPLLJ moisture fluxes are strengthened toward the NARR value. The impact of AN is also clearly seen in September when maximum NARR Great Plains fluxes move northward (Figs. 9d,p). AN simulation captures that shift, whereas the control maximum remains farther south near the CFS maximum.

Despite the model moisture flux biases, the simulated month-to-month changes, especially the low-level jets, are generally consistent with those of NARR. Even though observed NAM precipitation retreats in September, NARR poleward meridional moisture fluxes are strongest in September. Both RSM and CFS show September meridional moisture flux maximum, but September precipitation retreat is not as clear in the models (Fig. 5).

b. *NAM moisture budget and closure*

With maximum meridional moisture fluxes actually occurring within the NAM core region, it is worth examining the relative importance of regional recycling within the NAM core region and outside moisture sources. Stationary and transient moisture convergence into the NAME Tier 1 (or any arbitrary region) can be diagnosed as

$$-\int_{\text{box}} \nabla \cdot (\mathbf{F}+\mathbf{f})\, dA = -\oint_{\text{box}} (\mathbf{F}+\mathbf{f}) \cdot d\mathbf{N}. \qquad (4)$$

Equation (4) is area averaged for more standard units (mm day^{-1}):

$$\sum\left(\frac{\text{mm}}{\text{day}}\right) = \frac{-\oint_{\text{box}} (\mathbf{F}+\mathbf{f}) \cdot d\mathbf{N}}{A_{\text{box}} \cdot \rho_{H_2O(l)}} \times 86\,400\ \frac{\text{day}}{\text{sec}}. \qquad (5)$$

Since the box is defined along constant latitude and longitude, only fluxes normal to the boundary need to be calculated. Ideally, $\sum$ in Eq. (5) is equal to the area-averaged precipitation minus evaporation ($P - E$) by mass conservation:

$$\sum = \frac{\int_{\text{box}} (P-E)\, dA}{A_{\text{box}}}. \qquad (6)$$

Equation (6) does not hold for reanalyses because of data assimilation. For NARR, only P, $\mathbf{F}$, and $\mathbf{f}$ are nudged by data assimilation, with E as a rogue unconstrained variable (Nigam and Ruiz-Barradas 2006); E is the only variable that is not directly observable.

NARR, CFS, and RSM NAM moisture budgets are shown in Fig. 11. CFS-simulated $P - E$ and $\sum$ are negative and positive, respectively, meaning the simulated CFS NAM core region acts as a moisture source. Relative to NARR and CFS, RSM-simulated (both control and AN) $\sum$ and $P - E$ are close to naught, showing a relatively self-sustaining RSM NAM hydrological cycle.

NARR NAM water budget imbalances ($P - E - \sum$) are severe; moisture fluxes show net outside moisture convergence, yet $P - E$ shows the region as a moisture source. Imbalances in RSM are nearly comparable to those in CFS, with all models on the same order of magnitude (0.2–0.6 mm day^{-1}). NARR imbalances are an order of magnitude larger than the imbalances of the models (2.6 mm day^{-1}). Direct comparisons with NARR are difficult—evaporation and meridional moisture fluxes at the northern and southern boundaries are already well documented as having low confidence. All models and NARR agree in moisture transport over the Mexican highlands and in westward loss of moisture toward the open subtropical Pacific.

c. *Why the erroneous hydrological seasonal cycle?*

Understanding the NARR precipitation seasonal cycle within the context of NARR moisture budgets is not easy. The quality of NARR precipitation remains excellent under questionable moisture fluxes and surface evaporation. Observed surface evaporation (over land and water) is difficult to quantify simply because of the lack of in situ observations.

NARR handling of the GC SST is also questionable. To illustrate the differences in surface evaporation between NARR and the models, surface evaporation for July and August 2004 is plotted in Fig. 12. July and August 2004 are selected because there are ship surface flux measurements in the GC mouth from the NAME intense observational period. The impact of spurious NARR surface temperatures in the GC (Fig. 1) is evident in surface evaporation rates as well. Ship-measured surface evaporation in the GC mouth is approximately ~100 W m^{-2} (or ~3.5 mm day^{-1}; Fig. 8 in Zuidema et al. 2007). CFS and RSM surface evaporations in the lower GC are about half of NARR (NARR ~5–7 mm day^{-1}; models ~3–4 mm day^{-1}). Despite problematic handling of the GC in CFS, CFS evaporation is actually more realistic in certain parts of the GC. Over land, NARR surface evaporations are also higher than those of the models, especially near the United States–Mexico border; however, there are no in situ observations to verify the actual value.

Figure 11 shows that RSM- and CFS-simulated evaporation and moisture fluxes are behaving in a self-consistent manner. Understanding of the simulated erroneous NAM seasonal cycle can be carried out within the context of simulated moisture budgets. Shown in Table 1 are the monthly variations of NARR-, RSM-, and CFS-simulated moisture flux convergences and surface evaporations (divided between land and water, weighted by area fraction)

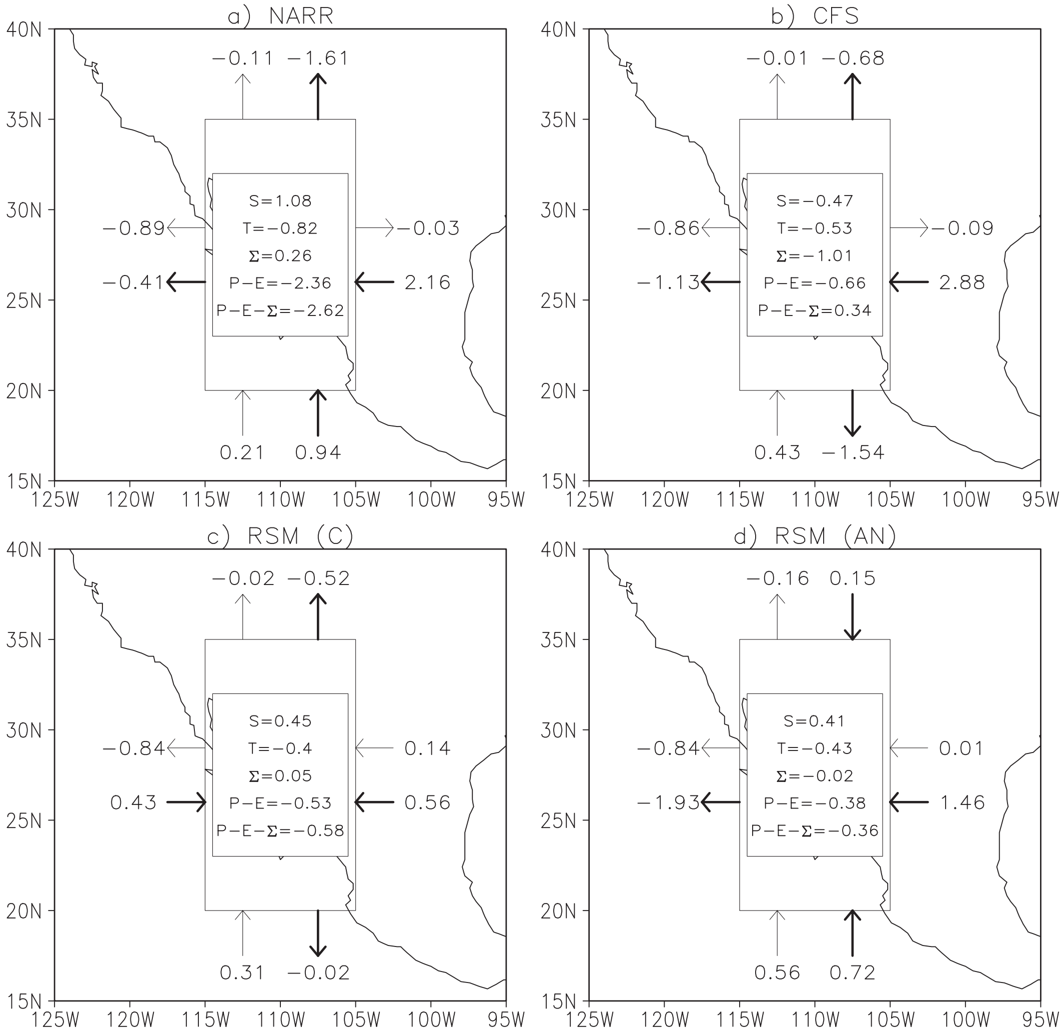

FIG. 11. A schematic showing moisture fluxes and balances for the NAME Tier 1 region. Thick and thin arrows indicate stationary and transient moisture fluxes from each side of the box, respectively. Arrows pointing inward with positive values indicate flux inward (convergent), while arrows pointing outward with negative values indicate flux outward (divergent). The residues for the stationary fluxes (S), transient fluxes (T), and their sum ($\sum = S + T$) are shown at the middle. For comparison, $P - E$ and its difference with $\sum$ are shown as well. All values are in mm day^{-1}.

within the NAM core region. The fractional area covered by water is shown as well. In general, evaporation over water is the leading term in NARR and in all three model predictions.

Moisture flux convergences and evaporation over water continue to increase into September. NARR September evaporation over land has decreased and is qualitatively reflecting the retreat of NAM precipitation (reduced rainfall leads to soil drying and reduced evaporation). Given the above analyses, and results from Mo et al. (2005) and Zuidema et al. (2007), erroneous NARR NAM moisture budgets (Fig. 11) appear to be a consequence of erroneous atmospheric moisture fluxes (both the seasonal mean and monthly variability) and air–sea interaction.

CFS- and RSM-simulated evaporation over land is comparable with that of NARR. Simulated evaporation over water continues to increase into September, but the increase is much more moderate than in NARR; simulated September values are about one-half to one-third of NARR values. With the exception of RSM (C), simulated NAM monthly moisture flux convergence continues to increase into September. The RSM (C) moisture flux convergence for September has decreased, but the decrease is moderate compared to the monthly variability of the other terms.

The true evaporation over water and land is unknown. Model-simulated evaporation over water is far less than that of NARR, at least over water within the NAM core

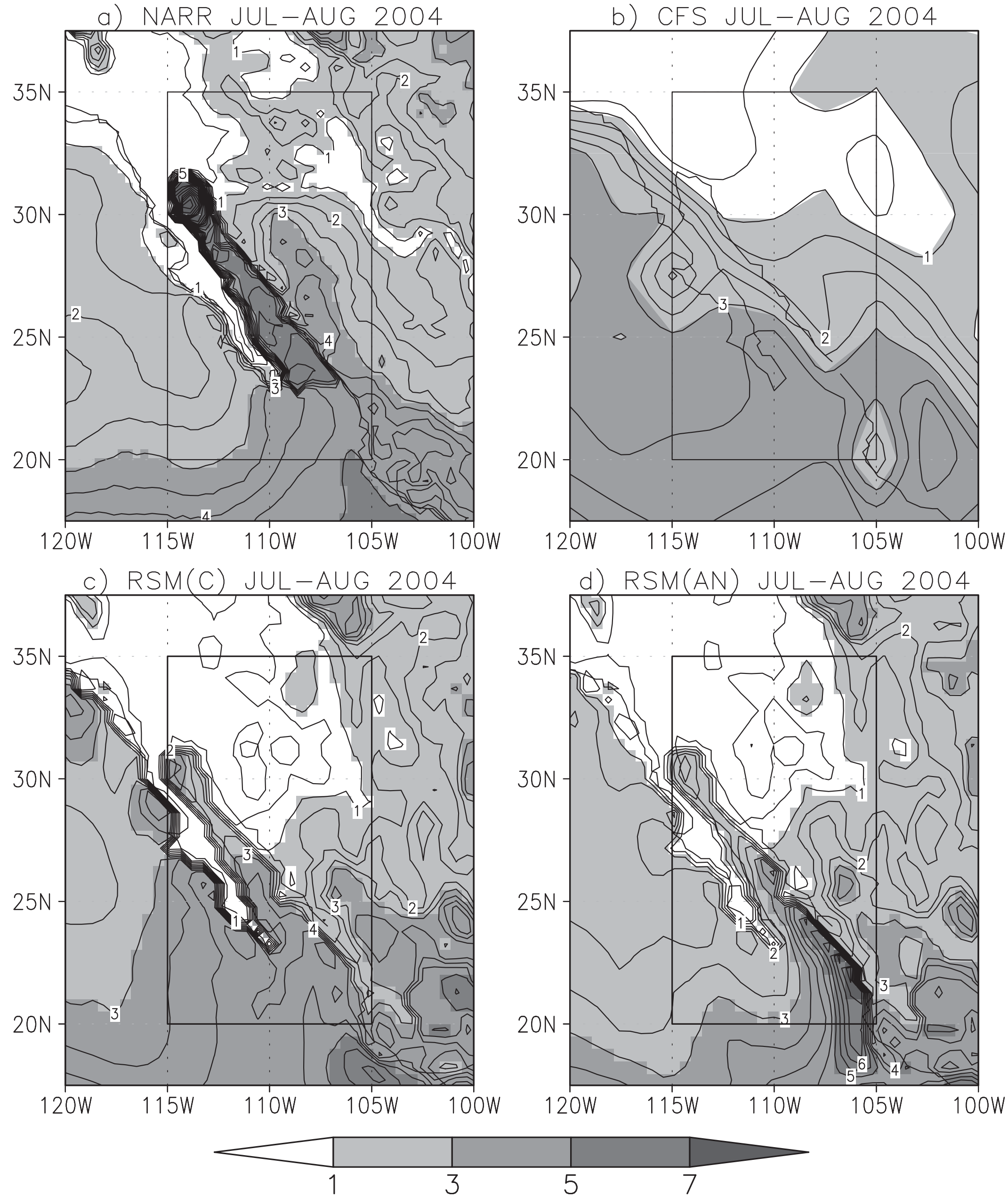

FIG. 12. Surface evaporation (mm day^{-1}) for July and August 2004 only—the month's ship-measured surface fluxes from the North American Monsoon Experiment field campaign are available. Contour intervals are every 0.5 mm day^{-1}.

region. This may be because CFS- and RSM-prescribed GC SST are strongly influenced by the cold SSTs in the California current because of the coarse resolution of the CFS (Fig. 2). Therefore, contributions of simulated GC evaporations in the model integrations probably tend toward the low side. The consistency in land evaporation between NARR and the models is reinforced by the relatively small seasonal precipitation biases over land within the core region (Fig. 4). The seasonal cycle of atmospheric moisture flux convergences coming from outside the NAM core region is responsible for the erroneously predicted NAM seasonal cycle. Ironically, the predicted seasonality of nonlocal moisture flux convergences agrees well with that of NARR, and the corresponding seasonality is similar in both the coarse- and fine-grid models—with and without bias correction (AN).

TABLE 1. The monthly variations of moisture flux convergences (stationary plus transient; left value, mm day^{-1}), evaporation over water (center value, mm day^{-1}), and evaporation over land (right value, mm day^{-1}) within the NAM core region for NARR, CFS, RSM (C), and RSM (AN). The evaporation rates over water and land are area weighted by multiplying by $A_{\mathrm{Water}}/0.5$ and $(1 - A_{\mathrm{Water}})/0.5$, respectively, in which A_{Water} is the fractional area covered by water (shown in bottom row).

	NARR	CFS	RSM (C)	RSM (AN)
June	+0.11/1.94/0.70	−1.36/2.46/0.75	−0.52/2.28/0.90	−0.11/1.75/1.13
July	+0.21/2.55/1.47	−1.18/2.72/1.21	−0.07/2.30/1.09	−0.10/1.94/1.16
August	+0.13/3.80/2.11	−1.00/3.16/1.63	+0.46/2.70/1.42	−0.02/2.29/1.43
September	+0.61/4.68/1.64	−0.49/3.15/1.46	+0.41/3.23/1.47	+0.15/2.44/1.45
A_{Water}	0.45	0.40	0.37	0.37

7. Discussion and conclusions

a. Overall intercomparisons

In terms of CFS- and RSM-predicted seasonal mean NAM precipitation, the errors are not excessive. The modeled mean RSM and CFS summer precipitation within the NAM core region is actually well simulated relative to the nearby regions. The RSM-simulated summer season precipitation outside the NAM core region is often poorer than that of CFS, especially for the Gulf Coast and in southern Mexico.

The NAM region has complex terrain and coastline that coarse-resolution models (such as the T62 CFS) are simply unable to resolve. The value of downscaling is most clear where such topographic and coastline errors are perceived to be important. Outside the NAM area, the value of downscaling is much more limited. AN impact is most clear in the LLJs, which CFS simulates poorly. The impacts are not always positive. AN-simulated seasonal mean poleward GCLLJ moisture fluxes are higher than those of NARR, and NARR GCLLJ moisture fluxes are already too high (Fig. 9). However, AN simulations are also the only simulations able to simulate a seasonal mean poleward stationary moisture flux. CFS and both RSM-simulated poleward transient fluxes are higher than those of NARR and contribute to nearly 45% of the AN poleward moisture fluxes. Considering the errors of NARR (and other reanalyses), as much work is needed for the reanalyses as for the models.

Both the RSM- and CFS-simulated NAM are negatively influenced by erroneous precipitation over eastern and southern Mexico. Poorly simulated NAM diurnal and seasonal variability can be explained entirely within the context of the erroneous precipitation over eastern and southern Mexico. Our analysis reveals the need to understand the American climate and monsoon system as a whole; the need for an accurate simulation of a broader region (such as NAME Tier 1.5–2) precedes the focus on a smaller region (NAME Tier 1).

Simulations of RSM and CFS are presented in Gutzler et al. (2009). Because reanalysis was downscaled in their study, RSM results presented in that paper cannot be compared directly with the RSM results presented here. Additionally, our results show that CFS has exhibited clear subseasonal monthly LLJ variability, which is closely tied with subseasonal monthly precipitation variability. In general, both CFS and RSM late NAM season rainfall is explained by the seasonal variability of moisture fluxes over the GC and the eastern Pacific.

b. Consequences of precipitation data assimilation

Why are the model-simulated nonlocal moisture flux convergences wrong? The impact of precipitation assimilation is not limited to the actual quality of the reanalysis precipitation. NARR divergent circulation and latent heating are nudged as a consequence of the precipitation data assimilation. Here, we compare the meridional moisture fluxes and precipitation forecasts of two additional reanalyses (Fig. 13): NCEP reanalysis I and the 40-yr European Centre for Medium-Range Weather Forecasts (ECMWF) Re-Analysis (ERA-40; Uppala et al. 2005).[3] Neither NCEP reanalysis I nor ERA-40 assimilates precipitation.

The NCEP reanalysis August–September change of precipitation forecasts and meridional moisture fluxes are similar to those of RSM and CFS; NAM rainfall and meridional moisture fluxes over the eastern Pacific continue to increase through September. The meridonal moisture flux increases are evident in ERA-40; the increases are more moderate and are mostly confined over land within the NAM region itself. Unlike NCEP reanalysis, ERA-40 successfully captures the retreat of September NAM precipitation.

There is one other subtle similarity between the model simulations (Fig. 5) with NCEP reanalysis I: the decrease of precipitation southeast of the NAM core region. That feature is absent in ERA-40. Precipitation translates to latent heating, and boreal summer NCEP reanalysis diabatic heating is higher than it is in ERA-40 over Central

[3] The years used by ERA-40 data are different, 1979–2001, as the dataset ends at August 2002. The plotted NCEP reanalysis I data cover the same year as the CFS and RSM simulations (June–September 2000–07).

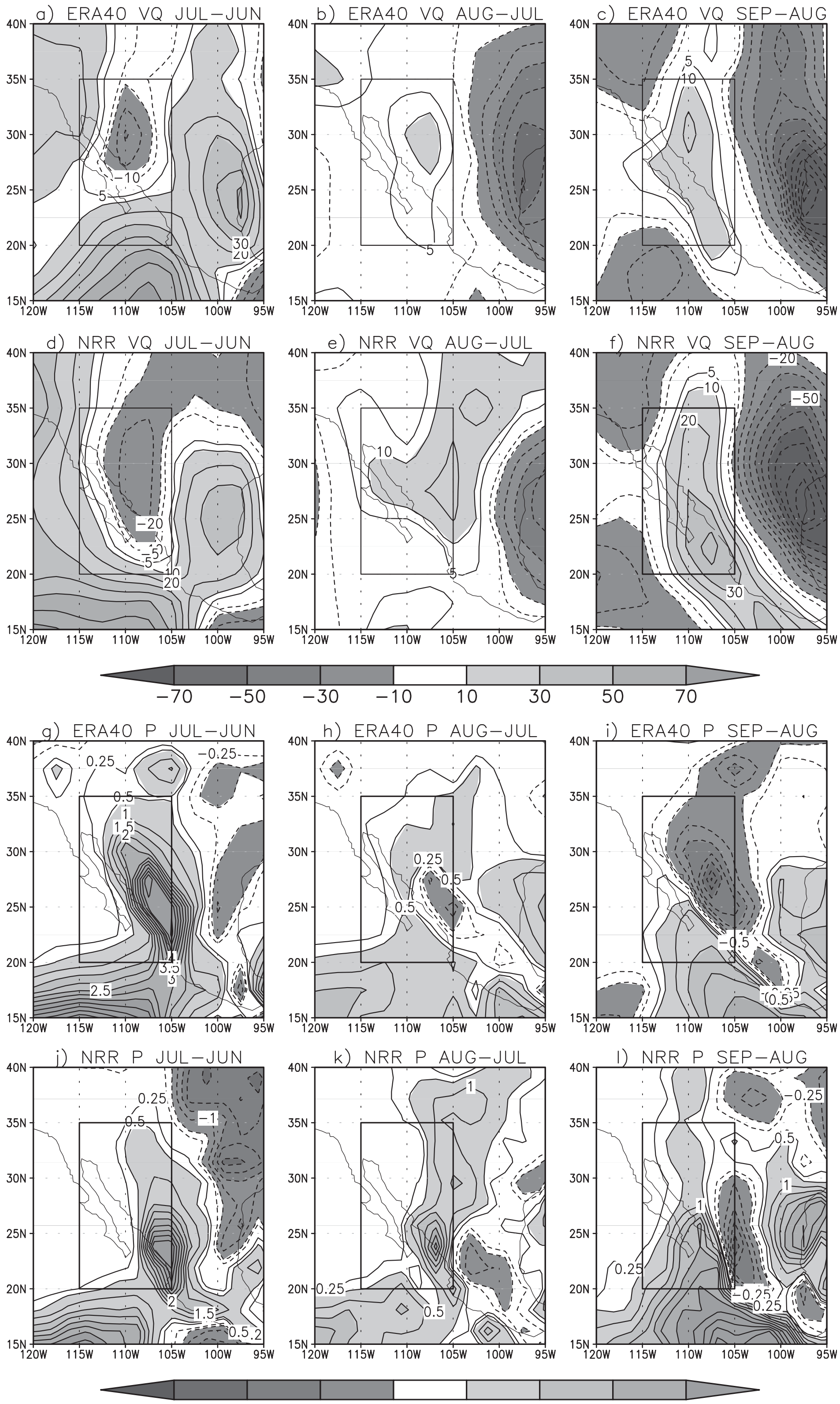

FIG. 13. Monthly change (as in Fig. 5) of (a)–(f) stationary meridional moisture fluxes {[$(\mathbf{F} + \mathbf{f}) \cdot \mathbf{j}$]; kg s^{-1} m^{-1}} and (g)–(l) precipitation (mm day^{-1}) for NCEP–NCAR reanalysis (NRR) and ERA-40.

America (Chan and Nigam 2009). The reduced September precipitation (reduction of atmospheric diabatic heating) produces poleward low-level flow acceleration to the west and northwest of the heat source (Rodwell and Hoskins 1996).

NARR has avoided the above heating error through precipitation assimilation. However, the NARR seasonal cycle of the moisture flux gives a contrasting NAM seasonal cycle. NARR meridional moisture fluxes are the highest, even higher than the models. Why is this the case? It may be noted that NARR's lateral boundary conditions include NCEP reanalysis II, so similarities between NARR and NCEP reanalysis moisture fluxes may not be just coincidental.[4] Considering NARR's relatively large moisture budget imbalance and erroneous GC air–sea interactions, has NARR avoided an erroneous NAM seasonal cycle by simply assimilating precipitation?

The above discussions provide evidence of why an increase in horizontal resolution may not guarantee simulation improvement. Errors in the global large-scale data (CFS and NCEP reanalysis) are expected to leave footprints in the regional simulations (RSM and Eta). Nudging and data assimilation have complicated the interpretation of the downscaled climate.

c. *Implications of and strategies for bias correction*

Our results show that downscaling and AN improve some of the seasonal mean dynamical fields (winds), most notably in the LLJs. Only the AN simulations have managed to produce a seasonal mean stationary moisture flux convergence into the NAM core region from the south (Fig. 11). However, when transient fluxes are added, AN moisture fluxes from the south are even higher than those of NARR. In fact, all models' transient moisture fluxes are higher than those of NARR.

AN bias corrections are not suitable for correcting monthly and diurnal variability errors as the correction is applied to the seasonal average in this study. Six-hourly/daily data for long-term CFS simulations are not readily available. It would be worthwhile to examine the efficacy of AN when diurnal rectification to the mean field is made.

Our analyses and literature review clearly indicate that the reanalysis seasonal cycles and means are often as erroneous and questionable as those produced in climate models. There are hints in our analysis that ERA-40 has a more realistic NAM representation than does NCEP reanalysis. Newer reanalysis products released since the introduction of ERA-40 await analysis. We see future research opportunities for regional and mesoscale model downscaling of bias-corrected global model simulations in which different reanalyses are used.

[4] A comparison (not shown) shows NCEP reanalysis II stationary meridional moisture fluxes to be even higher than those of NCEP reanalysis I.

d. *Value of downscaling from global models*

The imbalance between model moisture flux convergences and $P - E$ in the models is comparable to the spread of the flux convergences among models. Nigam and Ruiz-Barradas (2006) have shown that, despite significant moisture imbalance in NARR, it is an improvement over the reanalyses that do not assimilate rainfall.

CFS simulations of NAM are generally poor, and the regional model inherits those errors. In one sense, RSM does what regional models were originally intended for: it adds information and detail to the coarse-grid data (e.g., low-level jets and finer features of regional precipitation). However, regional models are not suitable for fixing a poor global model simulation. In fact, the most critical RSM errors can be explained in the context of CFS biases.

Acknowledgments. We kindly thank Scripps Institution of Oceanography–Experimental Climate Prediction Center for sharing RSM with us. We would also like to thank Meredith Field and Kathy Fearon of FSU COAPS for providing editorial assistance in preparing this manuscript. This research is supported by the NOAA Grant NA07OAR4310221 and USDA.

REFERENCES

Adams, D. K., and A. C. Comrie, 1997: The North American monsoon. *Bull. Amer. Meteor. Soc.,* **78,** 2197–2213.

Anderson, B., 2002: Regional simulation of intraseasonal variations in the summertime hydrologic cycle of the southwestern United States. *J. Climate,* **15,** 2282–2300.

——, and J. Roads, 2002: Regional simulation of summertime precipitation over the southwestern United States. *J. Climate,* **15,** 3321–3342.

——, and H. Kanamaru, 2005: The diurnal cycle of the summertime atmospheric hydrologic cycle over the southwestern United States. *J. Hydrometeor.,* **6,** 219–228.

——, ——, and J. Roads, 2004: The summertime atmospheric hydrological cycle over the southwestern United States. *J. Hydrometeor.,* **5,** 679–692.

Becker, E. J., and E. H. Berbery, 2008: The diurnal cycle of precipitation over the North American monsoon region during the NAME 2004 field campaign. *J. Climate,* **21,** 771–787.

Behringer, D. W., and Y. Xue, 2004: Evaluation of the global ocean data assimilation system at NCEP: The Pacific Ocean. Preprints, *Eighth Symp. on Integrated and Observation Systems for Atmosphere, Ocean, and Land Surface,* Seattle, WA, Amer. Meteor. Soc., 11–15.

Chan, S. C., and S. Nigam, 2009: Residual diagnosis of diabatic heating from ERA-40 and NCEP reanalyses: Intercomparisons with TRMM. *J. Climate,* **22,** 414–428.

Collier, J. C., and G.-J. Zhang, 2007: Effects of increased horizontal resolution on simulation of the North American monsoon in the NCAR CAM3: An evaluation based on surface, satellite, and reanalysis data. *J. Climate,* **20,** 1843–1861.

Douglas, A. V., and P. J. Englehart, 2007: A climatological perspective of transient synoptic features during NAME 2004. *J. Climate,* **20,** 1947–1954.

Ek, M. B., K. E. Mitchell, Y. Lin, P. Grunmann, E. Rogers, V. Koren, G. Ganyo, and J. D. Tarpley, 2003: Implementation of the upgraded Noah land surface model in the NCEP operational mesoscale Eta model. *J. Geophys. Res.,* **108,** 8851, doi:10.1029/2002JD003296.

Feldman, G. C., and C. R. McClain, cited 2010: Ocean color web. [Available online at http://oceancolor.gsfc.nasa.gov/.]

Gao, X., J. Li, and S. Sorooshian, 2007: Modeling intraseasonal features of 2004 North American monsoon precipitation. *J. Climate,* **20,** 1882–1896.

Gochis, D. J., W. J. Shuttleworth, and Z. Yang, 2002: Sensitivity of the modeled North American monsoon regional climate to convective parameterization. *Mon. Wea. Rev.,* **130,** 1282–1298.

——, C. J. Watts, J. Garatuza-Payan, and J. Cesar-Rodriguez, 2007: Spatial and temporal patterns of precipitation intensity as observed by the NAME event rain gauge network from 2002 to 2004. *J. Climate,* **20,** 1734–1750.

Gutzler, D. S., and Coauthors, 2009: Simulations of the 2004 North American monsoon: NAMAP2. *J. Climate,* **22,** 6716–6740.

Higgins, W., and D. Gochis, 2007: Synthesis of results from the North American Monsoon Experiment (NAME) process study. *J. Climate,* **20,** 1601–1607.

Holton, J. R., 1967: The diurnal boundary layer wind oscillation above sloping terrain. *Tellus,* **19,** 199–205.

Hong, S.-Y., and H.-L. Pan, 1996: Nonlocal boundary layer vertical diffusion in a medium-range forecast model. *Mon. Wea. Rev.,* **124,** 2322–2339.

——, and ——, 1998: Convective trigger function for a mass-flux cumulus parameterization scheme. *Mon. Wea. Rev.,* **126,** 2599–2620.

Janowiak, J. E., V. J. Dagostaro, V. E. Kousky, and R. J. Joyce, 2007: An examination of precipitation in observations and model forecasts during NAME with emphasis on the diurnal cycle. *J. Climate,* **20,** 1680–1692.

Johnson, R. H., P. E. Ciesielski, T. S. L'Ecuyer, and A. J. Newman, 2010: Diurnal cycle of convection during the 2004 North American Monsoon Experiment. *J. Climate,* **23,** 1060–1078.

Juang, H.-M., and M. Kanamitsu, 1994: The NMC nested regional spectral model. *Mon. Wea. Rev.,* **122,** 3–26.

Kalnay, E., and Coauthors, 1996: The NCEP/NCAR 40-Year Reanalysis Project. *Bull. Amer. Meteor. Soc.,* **77,** 437–471.

Kanamaru, H., and M. Kanamitsu, 2007: Scale-selective bias correction in a downscaling of global analysis using a regional model. *Mon. Wea. Rev.,* **135,** 334–350.

Kanamitsu, M., W. Ebisuzaki, J. Woolen, S.-K. Yang, J. J. Hnilo, M. Fiorino, and G. L. Potter, 2002: NCEP–DOE AMIP-II Reanalysis (R-2). *Bull. Amer. Meteor. Soc.,* **83,** 1631–1643.

Kirtman, B. P., D. A. Paolino, J. L. Kinter, and D. M. Straus, 2001: Impact of tropical subseasonal SST variability on seasonal mean climate simulations. *Mon. Wea. Rev.,* **129,** 853–868.

Lee, M.-I., and Coauthors, 2007: Sensitivity to horizontal resolution in the AGCM simulations of warm-season diurnal cycle of precipitation over the United States and Northern Mexico. *J. Climate,* **20,** 1862–1881.

Mahrt, L., and H.-L. Pan, 1984: A two-layer model of soil hydrology. *Bound.-Layer Meteor.,* **29,** 1–20.

Mesinger, F., and Coauthors, 2006: North American Regional Reanalysis. *Bull. Amer. Meteor. Soc.,* **87,** 343–360.

Misra, V., 2007: Addressing the issue of systematic errors in a regional climate model. *J. Climate,* **20,** 801–818.

——, and M. Kanamitsu, 2004: Anomaly nesting: A methodology to downscale seasonal climate simulations from AGCMs. *J. Climate,* **17,** 3249–3262.

——, L. Marx, M. Fennessy, B. Kirtman, and J. L. Kinter III, 2008: A comparison of climate prediction and simulation over the tropical Pacific. *J. Climate,* **21,** 3601–3611.

Mo, K. C., M. Chelliah, M. L. Carrera, R. W. Higgins, and W. Ebisuzaki, 2005: Atmospheric moisture transport over the United States and Mexico as evaluated in the NCEP regional reanalysis. *J. Hydrometeor.,* **6,** 710–728.

Nesbitt, S. W., D. J. Gochis, and T. J. Lang, 2008: The diurnal cycle of clouds and precipitation along the Sierra Madre Occidental observed during NAME-2004: Implications for warm-season precipitation estimation in complex terrain. *J. Hydrometeor.,* **9,** 728–743.

Nigam, S., and A. Ruiz-Barradas, 2006: Seasonal hydroclimate variability over North America in global and regional reanalyses and AMIP simulations: Varied representation. *J. Climate,* **19,** 815–837.

Rodwell, M. J., and B. J. Hoskins, 1996: Monsoons and the dynamics of deserts. *Quart. J. Roy. Meteor. Soc.,* **122,** 1385–1404.

Saha, S., and Coauthors, 2006: The NCEP climate-forecasting system. *J. Climate,* **19,** 3483–3517.

Smith, T. M., and R. W. Reynolds, 2004: Improved extended reconstruction of SST (1854–1997). *J. Climate,* **17,** 2466–2477.

Uppala, S., and Coauthors, 2005: The ERA-40 Re-Analysis. *Quart. J. Roy. Meteor. Soc.,* **131,** 2961–3012.

Wang, W., and P. Xie, 2007: A multiplatform-merged (MPM) SST analysis. *J. Climate,* **20,** 1662–1679.

Yang, S., Y. Jiang, D. Zheng, R. W. Higgins, Q. Zhang, V. E. Kousky, and M. Wen, 2009: Variations of U.S. regional precipitation and simulations by the NCEP CFS: Focus on the Southwest. *J. Climate,* **22,** 3211–3231.

Zuidema, P., C. Fairall, L. M. Hartten, J. E. Hare, and D. Wolfe, 2007: On air–sea interaction at the mouth of the Gulf of California. *J. Climate,* **20,** 1649–1661.